

Imaging phonons in a fcc Pu–Ga alloy by thermal diffuse x-ray scattering

Joe Wong,^{a)} M. Wall, and A. J. Schwartz

Lawrence Livermore National Laboratory, University of California, PO Box 808, Livermore, California 94551

R. Xu, M. Holt, Hawoong Hong, P. Zschack, and T.-C. Chiang

Frederick Seitz Materials Research Laboratory, University of Illinois at Urbana-Champaign, 104 South Goodwin Avenue, Urbana, Illinois 61801-2902 and Department of Physics, University of Illinois at Urbana-Champaign, 1110 West Green Street, Urbana, Illinois 61801-3080

(Received 18 November 2003; accepted 8 March 2004; published online 29 April 2004)

X-ray thermal diffuse scattering intensity patterns from phonons in a fcc δ -Pu–Ga alloy have been recorded using an 18 keV undulator x-ray beam with a beam diameter of 25 μm . The results are consistent with patterns calculated using the Born–von Karman force constant model of lattice dynamics, and support the pronounced softening of the transverse acoustic branch along the [111] direction observed from inelastic x-ray scattering measurements. This work demonstrates the feasibility of using a “large-grain, small beam” approach to study lattice properties, such as phonon dispersion curves, of materials not readily available in the form of large single crystals. © 2004 American Institute of Physics. [DOI: 10.1063/1.1737482]

The complex and often unique physical and metallurgical properties of plutonium (Pu) are well documented.¹ The pure metal exhibits six solid-state phases with large volume expansions and contractions along the path to the liquid state: $\alpha \rightarrow \beta \rightarrow \gamma \rightarrow \delta \rightarrow \delta' \rightarrow \epsilon \rightarrow \text{liquid}$. It melts at a relatively low temperature of $\sim 640^\circ\text{C}$ to yield a liquid with a density higher than that of the solid from which it melts. The fcc δ phase with a density of $\sim 15.8 \text{ g/cm}^3$ is 20% lower in density than the monoclinic α phase (19.86 g/cm^3), the latter being the stable phase at room temperature. The α phase, however, is brittle and difficult to handle by standard machining techniques. By alloying with a few percent of Group III metals such as Al and Ga, Pu can be retained in the δ phase over a wide temperature range around room temperature.^{2,3}

Lattice dynamical data (e.g., phonon dispersion curves, or PDCs) are critical to the understanding of the mechanical, electronic, and thermodynamic properties of Pu materials, including the interatomic force constants, sound velocities, elasticity, vibrational entropies, electron-phonon coupling, structural relaxation, phase stability, and phase transformations. However, measurements with conventional inelastic neutron scattering methods⁴ have been hindered by a high neutron absorption cross section of Pu and difficulties in growing single crystals large enough for neutron measurements. Thus, PDCs for Pu and its alloys have remained largely undetermined experimentally until recently.⁵ Theoretical calculations have proved to be difficult as well due to complications in treating the exchange and correlation effects associated with the 5f electrons, which can be either bonding or nonbonding, depending sensitively on the environment.^{1,6}

X-ray-based techniques provide attractive alternatives for phonon studies by avoiding the neutron absorption problem. Furthermore, x rays can be focused to a small spot size, allowing measurements to be performed on very small samples. With the high brightness third generation synchro-

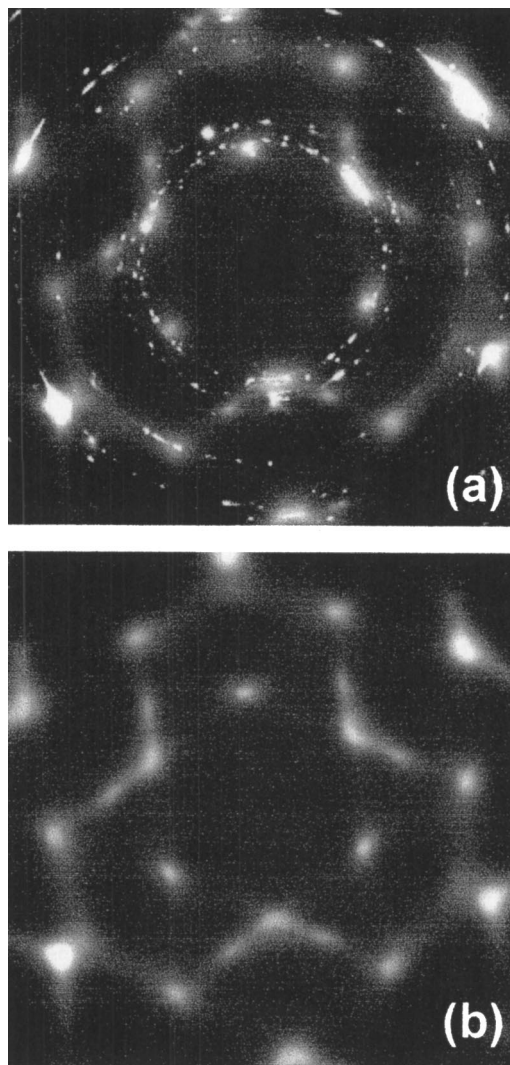


FIG. 1. Transmission TDS images from a fcc δ -Pu–Ga alloy along the [111] direction. (a) Experimental image obtained from a summation of 60 exposures, 30 s each. (b) Calculated image based on a Born–von Karman model with interactions to the fourth nearest neighbors. Both images are presented using a logarithmic intensity scale.

^{a)}Author to whom correspondence should be addressed; electronic mail: wong10@llnl.gov

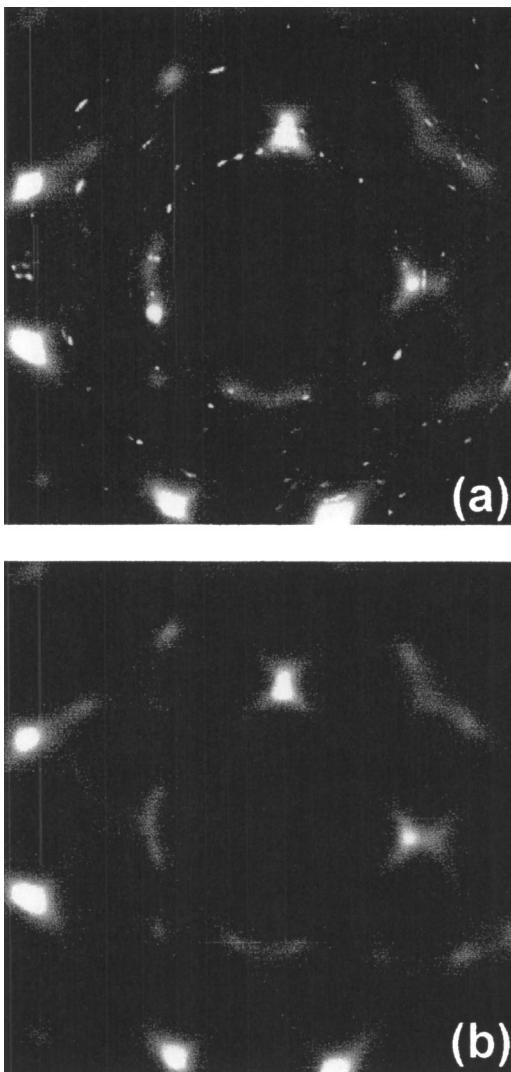


FIG. 2. Transmission TDS images from a fcc δ Pu-Ga alloy along the [100] direction. (a) Experimental image obtained from a summation of 100 exposures, 20 s each. (b) Calculated image based on a Born-von Karman model with interactions to the fourth nearest neighbors. Both images are presented using a logarithmic intensity scale.

tron sources, two powerful methods are now available. These are thermal diffuse scattering (TDS)⁷⁻⁹ and inelastic x-ray scattering.^{5,10-14} Aided by a recently developed technique for fabricating large-grain Pu materials,¹⁵ we have designed a TDS experiment and successfully measured patterns of x-ray scattering by thermal phonons in a fcc Pu-Ga alloy.

The material studied here is Pu with 0.6 wt% of Ga alloyed in for stabilization in the δ phase. The sample is 2.8 mm in diameter and about 30 μ m thick with grain sizes in the range of 50–100 μ m as determined by optical microscopy. The sample was mounted in an aluminum containment chamber in the form of a cylinder with a diameter of 70 mm, a height of 90 mm, and a wall thickness of 0.8 mm. These dimensions were chosen for an 18 keV beam to yield a desired maximum momentum transfer of $\sim 4 \text{ \AA}^{-1}$ (the lattice constant of the material is 4.621 \AA). An interior mounting plate and an external lead-disk beamstop were used, respectively, to prevent scattering from the upstream and downstream aluminum containment walls from reaching the detector. The containment chamber was needed both for safety reasons (Pu is highly radioactive and toxic) and for preserv-

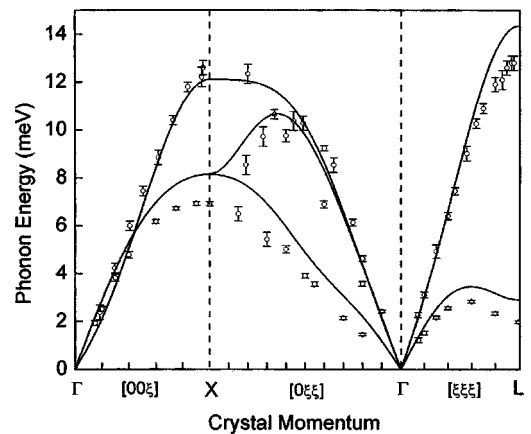


FIG. 3. Phonon dispersion curves of δ Pu-Ga. Open circles with error bars are inelastic x-ray scattering data (see Ref. 5). Solid curves are derived from a best fit to the TDS patterns based on a fourth nearest-neighbor Born-von Karman model.

ing sample integrity (Pu burns in air spontaneously and must be kept under an inert atmosphere at all times).

The TDS measurements were performed using the undulator beamline of UNICAT at the Advanced Photon Source (APS), Argonne National Laboratory, with the APS storage ring operating at 7 GeV and a current of 100 mA. The x-ray energy was set to 18.037 keV using a double Si(111) crystal monochromator. This energy is ~ 50 eV below the Pu L_3 edge, and the sample transmission is near a maximum with an absorption length of $\sim 14 \mu$ m. The incident beam was focused to $\sim 100 \mu$ m \times 260 μ m, and passed successively through a 0.5 mm \times 0.5 mm slit assembly and a pinhole to yield a 25- μ m-diam beam on the sample with an estimated flux of $\sim 6 \times 10^{10}$ photons/s. A transmission Laue geometry was employed, and the pattern of the scattered intensity was recorded by a charge coupled device (CCD) positioned immediately behind the sample containment chamber. The exposure times were typically in the range of 5–30 s. All measurements were performed with the sample at room temperature.

Area survey scans of scattering images were recorded systematically to map the single-crystal domains in the polycrystalline microstructure of the Pu-Ga specimen. The procedure consisted of scanning a 500 μ m by 500 μ m sample area with the 25 μ m beam using a step size of 50 μ m to yield a total of 121 scans. Each frame was visually examined to identify single-crystal domains. Of special interest were the (100), (111) and (110) domains with fourfold, threefold and twofold symmetry, respectively. Five such 500 μ m \times 500 μ m areas were mapped. We were successful in locating a number of (111)- and (100)-oriented grains, but could not find any (110) grains. At each located (111) and (100) grain, we performed a series of multiple exposures (60–100), with an exposure time of 20 or 30 s and the CCD operating at $\sim 50\%$ duty cycle. Each set of multiple scans was summed to give the final experimental TDS image.

Figure 1(a) is a transmission x-ray TDS image from a (111) grain. This image is obtained from a summation of 60 exposures, each for 30 s. Ignoring the Debye rings, the TDS pattern clearly exhibits threefold symmetry characteristic of the [111] direction. As is known from previous work,⁷⁻⁹ TDS patterns arise from x-ray scattering from thermally populated

TABLE I. Born–von Karman force constants to fourth nearest-neighbor interactions in N m^{-1} . The top row shows results from a direct fit to the PDCs of the same 0.6 wt% Ga–Pu alloy sample determined by inelastic x-ray scattering (see Ref. 5). The bottom row shows the results from a best fit based on a TDS analysis; the fit used the numbers in the top row as the initial input parameters.

1XX	1ZZ	1XY	2XX	2YY	3XX	3YY	3YZ	3XZ	4XX	4ZZ	4XY
9.409	-2.176	11.306	-3.097	0.905	-0.552	-0.295	-0.426	-0.324	-0.066	0.976	-0.498
9.152	0.739	11.650	-5.105	3.050	-0.765	-0.375	-1.711	-0.588	0.448	-0.583	0.058

phonons. Each point in the image corresponds to a unique momentum transfer. Regions in k space close to the reciprocal lattice points as defined by the Ewald sphere give rise to intense spots due to a high phonon population. Streaks connecting the intense spots are generally associated with high symmetry directions in the Brillouin zone. The image also shows the shadow of the beam stop. Shown in Fig. 1(b), for comparison, is a calculated TDS pattern based on a least-squares fit to the experimental results. The Debye rings have been indexed and can be shown to derive from microcrystalline δ -Pu–Ga (major phase) and PuO impurity (minor phase). The presence of these rings suggests that the best Pu–Ga samples currently available to us are not yet of sufficiently high quality for clean TDS work. The pattern shown in Fig. 1(a), however, indicates that the sample area illuminated by the x-ray beam ($25 \mu\text{m}$) is indeed essentially a single grain. Figure 2(a) is an experimental pattern from a (100) grain in the sample, obtained from a summation of 100 exposures, each for 20 s. Debye rings are also present. Ignoring these rings, the TDS pattern clearly exhibits fourfold symmetry characteristic of the [100] direction. The computed image, shown in Fig. 2(b), compares well with the experimental pattern.

The images shown in Figs. 1(b) and 2(b) are computed using the method discussed in detail in Ref. 9. Briefly, a Born–von Karman force constant model¹⁶ with interatomic force constants as input parameters is adopted to calculate the PDCs and the phonon polarization vectors. The x-ray scattering intensities are then computed and fitted to the two experimental images shown in Figs. 1(a) and 2(a) simultaneously with the interatomic force constants, the grain orientation, background, and overall normalization taken as adjustable fitting parameters. Force constants up to the fourth nearest neighbor are used. A difficulty here, not encountered in previous TDS studies,^{7–9} is the presence of Debye rings covering a significant portion of the images. An algorithm is employed in which a pixel is removed from the fit if its intensity is significantly higher than its neighbors. With this method we could take out most of the extraneous spots. However, the less intense spots and the TDS wings of the intense spots can still contaminate the fitting, resulting in errors in the final answer.

Indeed, fitting in the present case proved to be more problematic than previous TDS studies.^{7–9} Starting from various choices of initial parameters, several local minima in the χ^2 value were found. The best fits are shown in Figs. 1(b) and 2(b), and the corresponding phonon dispersion curves are shown in Fig. 3. Also shown in Fig. 3 (circles and error bars) are the experimental data determined by inelastic x-ray scattering.⁵ The agreement is clearly not as good as in previous studies of other systems^{7–9} due to the inferior sample quality in the present case. However, it is interesting to note that the present TDS analysis does reveal the phonon soften-

ing of the transverse acoustic branch near the L point. This is perhaps the most interesting feature of the Pu PDCs, and its temperature and pressure dependence is an important issue in regard to Pu science and technology. The interatomic force constants obtained from the best fit are listed in Table I. Also included in the table for comparison are the values deduced from a direct fit to the PDCs obtained from inelastic x-ray scattering. The differences can be taken to be an indication of the accuracy achievable with TDS from currently available samples.

In conclusion, the main purpose of the present TDS experiment on a fcc Pu–Ga alloy is to demonstrate the feasibility of a “*large-grain, small-beam*” approach in probing phonon properties of difficult materials that are not readily available in the form of large single crystals.

This work was performed under the auspices of the U.S. Department of Energy (DOE) by the University of California, Lawrence Livermore National Laboratory, under Contract No. W-7405-Eng-48 and by the University of Illinois Frederick Seitz Materials Research Laboratory under Grant No. DEFG02-91ER45439. The UNICAT facility at the APS is supported by the Frederick Seitz Materials Research Laboratory (U.S. DOE and the State of Illinois-IBHE-HECA), the Oak Ridge National Laboratory (U.S. DOE under contract with Lockheed Martin Energy Research), the National Institute of Standards and Technology (U.S. Department of Commerce), and UOP LLC. The APS is supported by the U.S. DOE, Office of Science, under Contract No. W-31-109-ENG-38.

¹Los Alamos Sci. **26**, 16 (2000).

²S. S. Hecker and L. F. Timofeeva, Ref. 1, pp. 244–251.

³S. S. Hecker, Ref. 1, pp. 290–335.

⁴G. Shirane, S. M. Shapiro, and J. M. Tranquada, *Neutron Scattering with a Triple-Axis Spectrometer* (Cambridge University Press, Cambridge, 2002), Chap. 4.

⁵J. Wong, M. Krisch, D. Farber, F. Occelli, A. Schwartz, T.-C. Chiang, M. Wall, C. Boro, and R. Xu, *Science* **301**, 1078 (2003).

⁶X. Dai, S. Y. Savrasov, G. Kotliar, A. Migliori, H. Ledbetter, and E. Abrahams, *Science* **300**, 953 (2003).

⁷M. Holt, Z. Wu, H. Hong, P. Zschack, P. Jemian, J. Tischler, H. Chen, and T.-C. Chiang, *Phys. Rev. Lett.* **83**, 3317 (1999).

⁸M. Holt, P. Zschack, H. Hong, M. Y. Chou, and T.-C. Chiang, *Phys. Rev. Lett.* **86**, 3799 (2001).

⁹M. Holt, P. Czochke, H. Hong, P. Zschack, H. K. Birnbaum, and T.-C. Chiang, *Phys. Rev. B* **66**, 064303 (2002).

¹⁰M. Krisch, A. Mermel, A. San Miguel, F. Sette, and C. Masciovecchio, *Phys. Rev. B* **56**, 8691 (1997).

¹¹M. Schwoerer-Böhning, A. T. Macrander, and D. Arms, *Phys. Rev. Lett.* **80**, 5572 (1998).

¹²E. Burkel, *Rep. Prog. Phys.* **63**, 171 (2000).

¹³F. Occelli, M. Krisch, P. Loubeyre, F. Sette, R. Le Toullec, C. Masciovecchio, and J.-P. Rueff, *Phys. Rev. B* **63**, 224306 (2001).

¹⁴H. Sinn, *J. Phys.: Condens. Matter* **13**, 7325 (2001).

¹⁵J. Lashley, M. G. Stout, R. A. Pereyra, M. S. Blau, and J. D. Embury, *Scr. Mater.* **44**, 2815 (2001).

¹⁶M. Born and K. Huang, *Dynamical Theory of Crystal Lattices* (Clarendon, Oxford, 1954).